第 48 卷 第 2 期/2021 年 1 月/中国激光 研究论文

中国激光

空间整形飞秒激光图案化加工氧化石墨烯

郭恒[1]，闫剑锋[1*]，李欣[2]，曲良体[1,3]

[1]清华大学机械工程系，北京 100084；

[2]北京理工大学机械车辆学院，北京 100081；

[3]清华大学化学系，北京 100084

摘要 氧化石墨烯(GO)是结构中含有部分含氧官能团的石墨烯衍生物，通过加热、化学反应和激光诱导等方法，该材料可以被还原。激光辐照可以诱导一定区域内的 GO 发生还原反应，具有灵活、区域选择性良好、无需特殊环境等优点。提出了一种基于空间整形的飞秒激光图案化加工 GO 的方法，即空间整形激光辐照法，分别采用空间整形激光辐照法和激光逐点扫描法在 GO 上加工图案，并对加工结果进行表征和对比，分析了辐照时间、激光通量等参数对加工结果的影响。结果表明空间整形激光辐照法可以图案化加工 GO 并使加工区域的 GO 被还原，从而提高图案化加工效率，且该方法具有良好的可重复性和图案灵活性，在制备 GO 基底的微电路、微器件方面具有应用潜力。

关键词 激光技术；飞秒激光；空间光整形；氧化石墨烯；图案化加工

中图分类号 TN249 **文献标志码** A **doi**：10.3788/CJL202148.0202018

1 引 言

石墨烯是一类重要的二维材料，自被发现以来引起了大量关注，具有优良的机械性能、高导电性和导热性等，已被广泛应用于多个领域[1]。制备高质量的石墨烯具有很大挑战性，目前常用的制备方法包括机械剥离石墨[2]、化学气相沉积[3]、外延生长[4]等。氧化石墨烯(GO)是一大类带有羟基、环氧和羧基等含氧官能团的石墨烯衍生材料[5]，其碳层结构中大量的 sp^2 碳碳键转化成为 sp^3 键，其性质不同于石墨烯[6]。诱导 GO 还原是制备类石墨烯材料的重要途径[7]，还原方法有化学还原[8]、热还原[9]和激光诱导还原[10]等，其中激光诱导还原法具有较好的灵活性和区域选择性。飞秒激光、纳秒激光和连续激光均可以诱导 GO 的还原，飞秒激光的效率更高[11]。飞秒激光还原 GO 包括两个过程，分别是碳碳键从 sp^3 键向 sp^2 键的转化和氧原子的去除[12]。飞秒激光逐点扫描可以在 GO 上加工微电路以实现线路电阻可调[13]，也可以在 GO 上制备不同形状的超级电容，从而使 GO 在能量存储方面具有一定的应用潜力[14]，GO 在生物、传感、催化等领域也有所应用[15-16]。

在诱导 GO 还原时，激光逐点扫描法的加工效率低，加工大量重复图案耗时长。激光空间整形技术可以改变焦点处光场的分布，从而提升加工效率、优化加工结果，利用经过空间整形的飞秒激光可在电介质、金属等材料上进行图案化加工[17-19]。衍射光学元件(DOE)可以将飞秒激光整形为多光束光场，用于在材料上快速制备相似图案[20]。数字微镜装置(DMD)通过加载特定相位图对激光进行光场整形，可以获得具有特殊功能的光场[21]。空间光调制器(SLM)具有使用便利、可重复使用、对光场利用率高等优点，在飞秒激光微纳加工领域有着广泛的应用[22]，其可以产生类型丰富的特殊光场，例如贝塞尔光束、艾里光束等，也可以产生任意图案化的光场，因此 SLM 在图案化加工方面具有应用潜力[23-24]。

本文采用空间整形的飞秒激光辐照 GO 表面，

收稿日期：2020-08-19；**修回日期**：2020-09-21；**录用日期**：2020-10-27

基金项目：国家重点研发计划(2017YFB1104300)、国家自然科学基金(51775303，52075289)

*E-mail：yanjianfeng@tsinghua.edu.cn

实现了对加工区域的还原图案化，这种加工方法称为空间整形激光辐照法。该方法根据 Gerchberg-Saxton(G-S)算法计算整形所需的相位图[25]，使用 SLM 加载相位图，对飞秒激光进行空间整形，使聚焦后的光场形状与待加工图案一致，通过定点辐照进行加工。作为对比的激光逐点扫描法可保持聚焦后光场的形状为点状，通过移动平移台使焦点扫过样品表面产生加工效果。文中分别采用空间整形激光辐照法和激光逐点扫描法加工 GO，使用扫描电镜、白光干涉仪和拉曼光谱仪对加工区域的微观形貌、成分信息进行表征和分析。结果表明，空间整形的飞秒激光辐照法可以对 GO 进行图案化加工，并具有较好的灵活性和可重复性，其图案化加工效率有所提升，在制备 GO 基底的微电路和微器件方面有广泛的应用前景。

2 实验过程

2.1 空间整形飞秒激光加工系统

本文使用的材料是通过抽滤、干燥 GO 分散液的方法获得的 GO 薄膜[26]，使用的飞秒激光波长为 800 nm，脉冲宽度为 35 fs，重复频率为 1 kHz。图 1(a)是飞秒激光空间整形及加工系统的示意图，衰减片和光阑用于调整飞秒激光的功率和光斑大小，电控快门用于控制激光辐照时间，平移台用于移动 GO 样品，使用的聚焦物镜为放大倍率为 5 的物镜，数值孔径(NA)为 0.15。通过迭代计算获得相位图之后，将相位图加载到透镜前焦面的 SLM 上，使透镜后焦面的光场分布成为目标形状并与需要加工的图案一致。为保证相位调制后的光场在传播过程中不失真，使用光学 $4f$ 系统将光场映射至聚焦物镜的入瞳处，经物镜聚焦后，将 GO 的表面定位在物镜焦面，通过定点辐照 GO 表面加工图案，并通过调整激光的通量和辐照时间改变加工效果。

在 SLM 上加载平面相位时，SLM 上所有像素点均保持相同的灰度值，此时的 SLM 相当于一个平面反射镜，不会改变激光束的高斯分布，在这样的状态下，在物镜焦点处可得到点状光场，并可以进行激光逐点扫描。控制平移台按照设计的路线平移，可以在 GO 表面加工图案，通过调整激光功率和扫描速度可以改变加工效果。

2.2 基于 SLM 的激光空间整形原理

激光空间整形技术主要基于透镜的衍射规律，以复振幅分布来表示光场，在透镜的前焦面上，光场可以表示为

$$U_0(x_0,y_0)=A_0(x_0,y_0)\exp[\mathrm{j}\varphi_0(x_0,y_0)], \tag{1}$$

式中：(x_0,y_0)为透镜前焦面上一点的坐标；$U_0(x_0,y_0)$表示透镜前焦面的光场分布；$A_0(x_0,y_0)$表示光场的振幅分布；$\varphi_0(x_0,y_0)$表示光场的相位分布。

根据透镜的菲涅耳衍射积分和相位变换规则，透镜后焦面的光场复振幅分布 $U(x,y)$和 $U_0(x_0,y_0)$的关系为

$$U(x,y)=C\iint U_0(x_0,y_0)\times \exp[-\mathrm{j}2\pi(\xi x_0+\eta y_0)]\mathrm{d}x_0\mathrm{d}y_0, \tag{2}$$

式中：(x,y)为透镜后焦面上一点的坐标；$U(x,y)$表示透镜后焦面的光场分布；C 为常数；ξ 和 η 为分别与 x 和 y 轴方向垂直的坐标。

由(2)式推导可知，$U(x,y)$是 $U_0(x_0,y_0)$的傅里叶变换(FT)结果，改变 $U(x,y)$的分布可以通过改变 $U_0(x_0,y_0)$来实现。根据(1)式，通过调整 $\varphi_0(x_0,y_0)$可以改变 $U_0(x_0,y_0)$，将 SLM 安装在透镜的前焦面，可以实现对前焦面光场相位分布的调制。

激光空间整形需要根据目标光场的复振幅分布 $U(x,y)$获得对应的相位分布 $\varphi_0(x_0,y_0)$，实现该过程的方法是 Gerchberg-Saxon 算法[25]，其示意图如图 1(b)所示。该算法为迭代算法，在首次迭代时，使用普通高斯分布的振幅和随机分布的相位来表示最初的光场复振幅分布 U_0。对此进行分步傅里叶

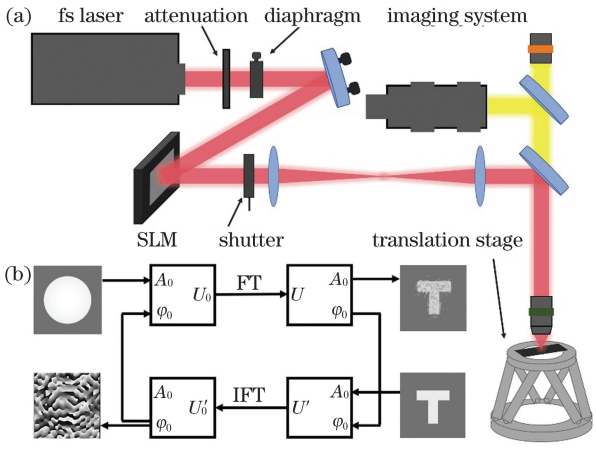

图 1 基于 SLM 的飞秒激光空间整形、加工光学系统及计算相位图的算法。(a)飞秒激光空间整形、加工光学系统；(b)G-S 迭代算法的示意图

Fig. 1 SLM-based optical system for space shaping and processing of femtosecond laser, and phase calculation algorithm. (a) Optical system for space shaping and processing of femtosecond laser; (b) schematic illustration of G-S iteration algorithm

变换，以获得新的光场分布 U。通常情况下，该光场分布与目标的光场形状相差很大，用目标光场的振幅代替 U 的振幅，保持计算出的相位不变，得到新的光场分布 U'。对 U' 进行傅里叶逆变换(IFT)，获得分布 U_0'，然后用初始高斯分布的振幅代替 U_0' 的振幅，保持计算出的相位不变，得到下次迭代的 U_0。按照此规律执行迭代 200 次，光场 U 几乎不再随着迭代次数的增加而变化，此时最新计算得到的 U_0' 的相位分布即为光场整形所需的相位分布。

2.3　加工区域表征实验

对样品进行还原图案化加工之后，使用扫描电镜对图案化区域进行表征，观察两种加工方法的图案化加工效果和微观形貌；使用白光干涉仪对加工区域的深度和均匀性进行表征；使用拉曼光谱仪获取图案化加工区域的拉曼光谱，根据拉曼光谱的特征峰的位置判断 GO 被飞秒激光还原的程度[11-12]。

3　分析与讨论

图 2 是空间整形激光辐照法和激光逐点扫描法在 GO 表面加工 4 个 40 μm×40 μm 正方形图案的结果对比。图 2(a)左右两侧分别显示了两种加工方法中在 SLM 上加载的相位图及焦点光场形状。当 SLM 上加载的是根据 G-S 算法计算出的相位图匀，为了便于表述，在计算飞秒激光通量时假设光场是均匀的。这里使用的激光通量为 0.156 J/cm^2，辐照时间为 500 ms。结果显示，加工的图案被沟壑状的结构分割成若干不规则区域，沟壑结构围绕着的区域形成了凸起结构，这些结构的产生是由光场分布不均匀导致的，沟壑结构对应于光场中的强光强部分，凸起结构对应于光场中的低光强部分，凸起结构的长度为 5～10 μm，今后可以通过对算法的进一步优化提高相位图的精细程度，从而提高光场分布的均匀性。凸起结构的边缘不光滑，有很多微小的层状结构，这是由于激光辐照过程中，GO 的含氧官能团与激光相互作用，短时间内产生大量 CO_2、CO 等气体，这些气体在 GO 的空隙中无法存储，快速释放出来，使得 GO 的结构变得疏松，产生层状结构。图 2(c)显示了激光逐点扫描法加工区域的微观形貌电镜照片及局部放大图，激光通量为 0.236 J/cm^2，扫描速度为 10 μm/s，扫描间隔为 1 μm。采用激光逐点扫描法加工的区域均匀和一致性更好，扫描加工的区域也存在凸起和沟壑结构，凸起结构的长度为 1 μm 左右，层状结构则在图案的边缘存在，这些微观形貌的相似性说明在两种加工方式中，激光与 GO 作用的过程是相似的。采用两种方法加工得到的微观形貌的区别在于激光逐点扫描法加工区域存在大

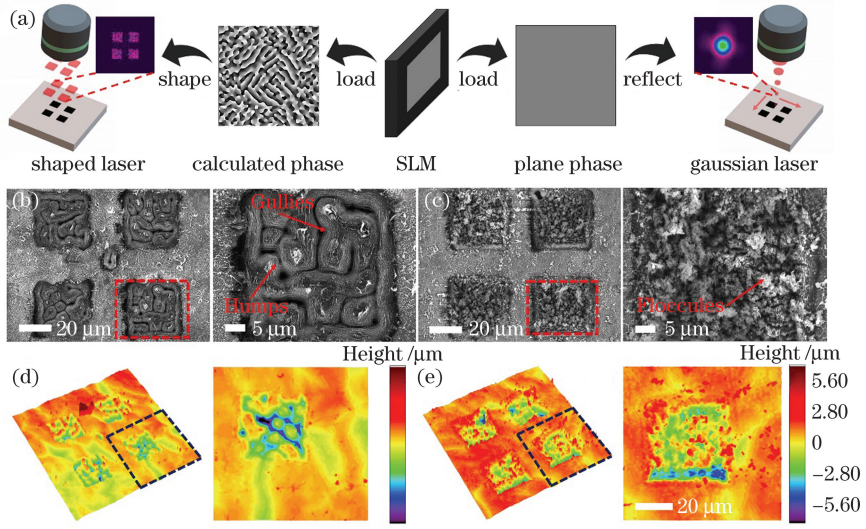

图 2　两种方法加工结果的对比。(a)在 SLM 上加载的不同相位及获得的不同光场分布(加载计算得到的相位获得整形激光，加载平面相位获得高斯激光)；(b)空间整形激光辐照区域的微观形貌；(c)激光逐点扫描区域的微观形貌；(d)空间整形激光辐照区域的深度分布；(e)激光逐点扫描区域的深度分布

Fig. 2　Comparison of processing results of two methods. (a) Two phases loaded on SLM and corresponding optical field distributions (load calculated phase to obtain spatially shaped laser and load plane phase to obtain Gaussian laser); (b) micromorphology of region irradiated by spatially shaped laser; (c) micromorphology of region for laser point-by-point scanning; (d) height distribution of spatially shaped laser irradiated pattern; (e) height distribution of region for laser point-by-point scanning

量絮状结构，这些絮状结构是扫描加工过程中 GO 被烧蚀喷发出的碎屑沉积在之前的加工区域产生的。经过计算可得，空间整形激光辐照法制备这一图案需要 500 ms，激光逐点扫描法需要 640 s，这说明空间整形激光辐照法可以提升图案化加工 GO 的效率。

图 2(d)和(e)是使用白光干涉仪对两种方法所加工区域深度分布的表征结果。图 2(d)显示了空间整形激光辐照法加工区域的深度分布，辐照区域内凸起结构的深度接近未加工区域，沟壑结构的深度达到 1～3 μm。图 2(e)显示了激光逐点扫描法加工区域的深度分布，总体上其深度分布均匀性优于空间整形激光辐照法加工的区域，但有一些颗粒状凸起分散在区域内，在最后加工的部分，颗粒状凸起明显减少，深度有所增加。颗粒状凸起就是微观形貌电镜图中所见的絮状结构，这些结构是扫描过程中由于烧蚀产生的碎屑在已加工区域中的沉积造成的，因此最后加工的部分因为没有碎屑沉积而成为整个区域中颗粒状凸起最少、深度最大的部分。

图 3 显示了采用空间整形激光辐照法加工时，不同激光通量和辐照时间对加工结果的影响。图 3(a)是空间整形激光在不同的激光通量和辐照时间下加工的正方形图案的微观形貌。在相同的激光通量下，当辐照时间从 500 ms 增加到 3000 ms，图案的微观形貌都是相似的，在相同的辐照时间下，当激光通量从 0.109 J/cm^2 增加到 0.204 J/cm^2，沟壑结构的宽度和深度明显增大。图 3(a)中虚线标记了一些加工结果中部分沟壑结构的位置和形状，不同参数组合对应的结果中沟壑结构的位置和形状一致，这说明使用相同的相位图能得到相同的加工图案，这也显示了空间整形激光辐照法具有良好的可重复性。图 3(b)是当激光通量为 0.156 J/cm^2，辐照时间从 0 ms 增大到 3000 ms 时空间整形激光辐照区域的拉曼光谱，辐照区域不均匀，选择平整区域作为拉曼光谱表征区域。拉曼光谱结果是以 G 峰强度 I_G 为基础进行标准化处理之后得到的[11]，D 峰强度 I_D 可以衡量 GO 的缺陷程度，2D 峰的强度 I_{2D} 与石墨烯的层数相关[12]。拉曼光谱的 D 峰强度和 G 峰强度之比 I_D/I_G 可以表示 GO 碳层结构的畸变程度，2D 峰强度和 G 峰强度之比 I_{2D}/I_G 可以表示 GO 被还原为石墨烯的程度。图 3(c)是根据图 3(b)的信息计算出的，显示了当激光通量为 0.156 J/cm^2 时，I_D/I_G 和 I_{2D}/I_G 随着辐照时间的

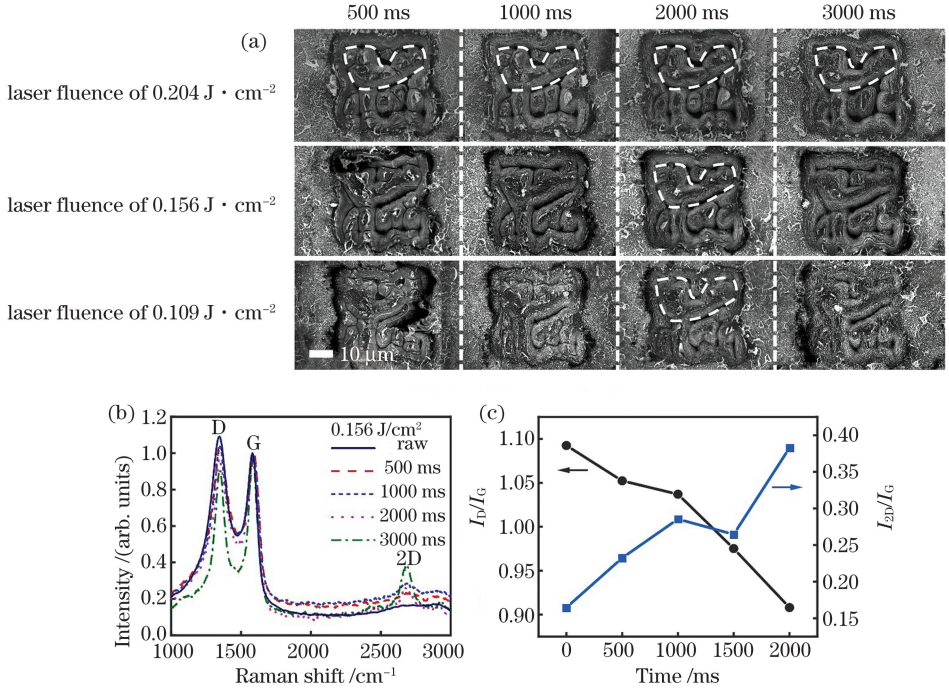

图 3　不同辐照时间和激光通量下空间整形激光辐照法的加工结果。(a)不同辐照时间和激光通量下辐照加工结果的微观形貌；(b)加工区域的拉曼光谱(以 G 峰强度为基础进行归一化)；(c) I_D/I_G 和 I_{2D}/I_G 随时间的变化趋势

Fig. 3　Processing results of spatially shaped laser irradiation method under different irradiation time and laser fluence. (a) Micromorphology of processing results under different irradiation time and laser fluence; (b) Raman spectra of processed regions (normalized based on intensity of peak G); (c) variations of I_D/I_G and I_{2D}/I_G with irradiation time

延长的变化趋势，在实验参数范围内，随着辐照时间的延长，I_D/I_G 减小，I_{2D}/I_G 增大，这表明在一定范围内，当激光通量相同时，更长的辐照时间有利于 GO 的还原。

图 4 是不同激光通量和扫描速度下，激光逐点扫描法加工的实验结果。图 4(a)显示在相同的激光通量下，当扫描速度从 5 μm/s 增加到 50 μm/s 时加工结果的形貌是相似的。当激光通量为 0.079 J/cm^2 时，扫描区域颜色变深，没有出现明显的形貌变化，随着激光通量的增加，凸起结构逐渐出现，絮状结构出现并增多、互相连接。图 4(b)是未经处理的 GO 和 5 μm/s 的扫描速度下，激光通量从 0.079 J/cm^2 增大到 0.315 J/cm^2 时激光逐点扫描区域的拉曼光谱结果。图 4(c)是根据图 4(b)的信息计算出的结果，显示了 5 μm/s 的扫描速度下，I_D/I_G 和 I_{2D}/I_G 与激光通量的变化关系。在实验参数范围内，激光通量增大时，I_D/I_G 减小，I_{2D}/I_G 增大，这表明在一定范围内，更大的激光通量有助于 GO 的还原。从两种方法的加工区域的拉曼光谱结果可以看出，两种加工方法对 GO 的最大还原程度是接近的，I_D/I_G 为 0.82～0.90，I_{2D}/I_G 为 0.35～0.38，达到类似的还原程度，两种加工方式所消耗的时间不同，空间整形激光辐照法所消耗的时间为 3 s，激光逐点扫描法所消耗的时间为 1280 s，这说明在进行 GO 的图案化加工并进行还原时，采用激光空间整形技术可以使加工效率得到显著提升。GO 是电介质材料，其带隙大小随着含氧官能团的含量的变化而变化，一般为 2.8～4.6 eV[27]。当扫描使用的激光通量低于 0.079 J/cm^2 时，无法产生明显的加工效果，这说明激光通量过低时不能对 GO 进行还原或烧蚀。当激光通量增大到可以还原 GO 时，GO 被还原，局部形成还原氧化石墨烯(rGO)，其带隙减小，烧蚀阈值降低，烧蚀和还原同时发生，故加工之后图案化区域的深度变化是还原和烧蚀同时出现的结果。空间整形激光辐照法同样存在激光通量越大则加工区域深度越大的规律，这也是还原和烧蚀同时出现的结果。

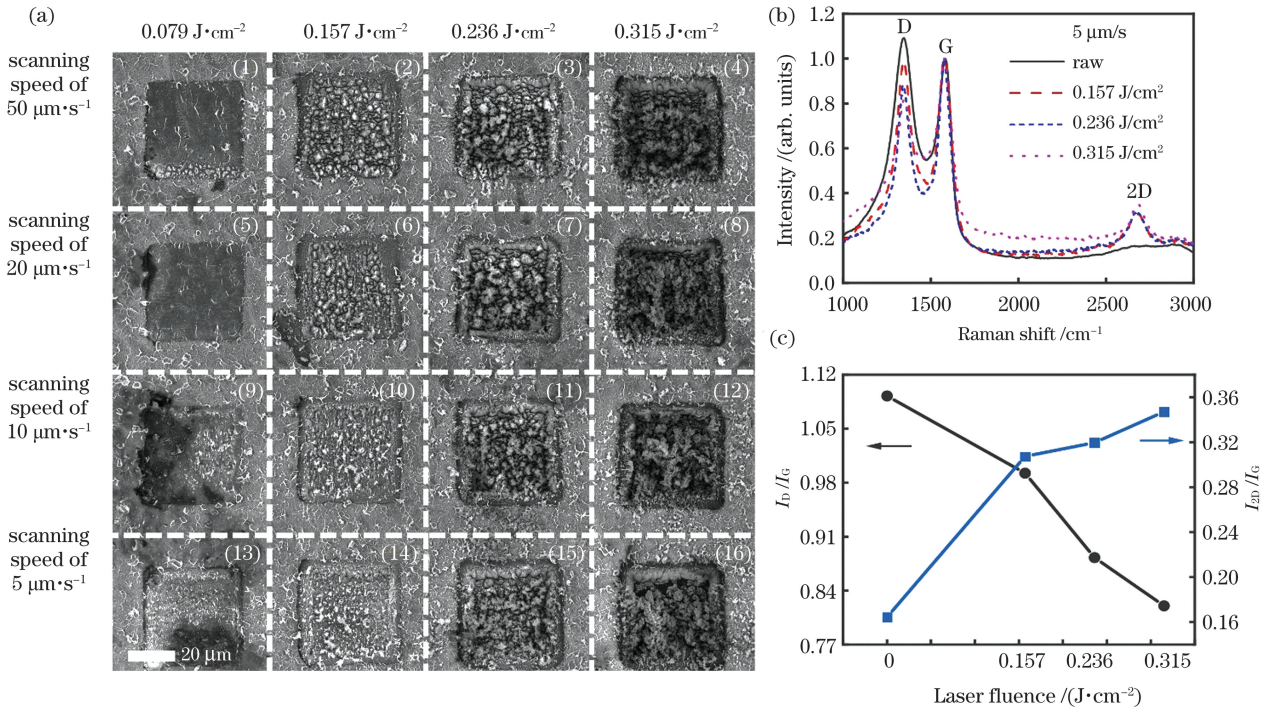

图 4 不同激光通量和扫描速度下的激光逐点扫描法加工结果。(a)不同激光通量和扫描速度下加工区域的微观形貌；(b)不同通量的激光扫描后的拉曼光谱结果；(c) I_D/I_G 和 I_{2D}/I_G 随激光通量的变化趋势

Fig. 4 Laser point-by-point scanning results under different laser fluence and scanning speed. (a) Micromorphologies of processed region for different fluence and scanning speed; (b) Raman spectra after scanning by laser under varying fluence; (c) variations of I_D/I_G and I_{2D}/I_G with laser fluence

图 5 是空间整形激光辐照法制备字母缩写“THU”图案的过程和结果。对于复杂的图案，相位图的求解计算量大，难以通过一次辐照获得完整的图案，可以采取分割组合的方法。在加工字母“THU”形图案时，可以先将图案分割为三个部分，分别求解对应的相位图并将其加载至 SLM 上，依

次在 GO 表面辐照产生加工效果。图 5(a)分别是“T”、“H”和“U”形图案对应的相位图，将相位图依次加载到 SLM 上，根据菲涅耳衍射规律计算的焦点处光场分布如图 5(b)所示[17]，可见光场分布呈现对应字母的形状。图案的微观形貌如图 5(c)所示，加工每个字母时在 GO 上定点辐照 500 ms，激光通量设置为 0.481 J/cm^2。图 5(d)和图 5(e)是对图 5(c)中字母图案的局部放大，可以看出加工区域内存在沟壑结构和凸起结构，凸起结构上存在层状微结构，这些结构产生的原因与前述原因一致。加工结果表明，使用分割图案、分区域求解相位图的方法可以降低相位图的计算难度，从而增强空间整形激光辐照法的图案化加工灵活性。

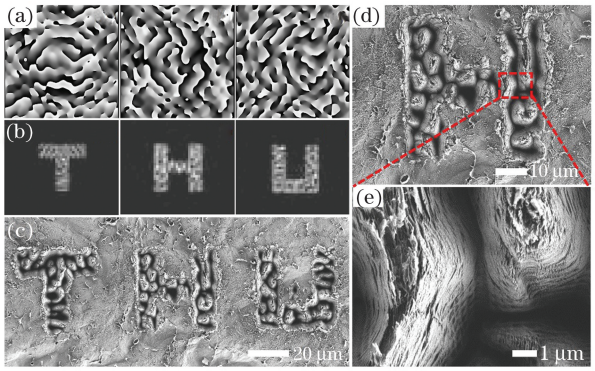

图 5 空间整形激光辐照法得到的字母图案。(a)三个字母对应的相位图；(b)根据三个相位图计算的焦点处光场分布；(c)～(e)辐照加工的三个字母的微观形貌及局部放大图

Fig. 5 Patterns of three letters fabricated by spatially shaped laser irradiation. (a) Phases corresponding to three letters; (b) simulated optical fields at focused point corresponding to three phase patterns; (c)-(e) micromorphologies of three letter patterns obtained by spatially shaped laser irradiation and local amplification maps

4 结 论

本文实现了一种基于激光空间整形技术对氧化石墨烯进行还原图案化加工的方法，即空间整形激光辐照法。通过比较空间整形激光辐照法和激光逐点扫描法，发现使用两种方法得到的加工区域的微观形貌不同，空间整形激光辐照法可以减少加工过程中碎屑堆积的现象。加工区域的微观形貌表明空间整形激光辐照法加工的图案具有良好的可重复性，如果 SLM 加载的相位图不发生变化，则多次加工产生的图案一致。两种加工方法均对 GO 有还原效果，在实验参数范围内，对于空间整形激光辐照法，长辐照时间和高激光通量有助于提高还原程度，而对于激光逐点扫描法，低扫描速度和高激光通量有助于 GO 的还原。进行还原图案化加工时，空间整形激光辐照法需要的时间少于激光逐点扫描法，这表明采用空间整形技术可以使图案化加工 GO 的效率提升。对加工图案进行合理的分割，使用空间整形飞秒激光进行分区域加工可以得到形状更复杂的图案，这显示了该方法较好的图案灵活性。空间整形激光辐照法对 GO 进行还原图案化加工时具有较好的可重复性和图案灵活性，且图案化加工效率得到提升，该方法在制备 GO 基底微电路、微器件等方面具有广泛的应用前景。

参 考 文 献

[1] Novoselov K S, Fal'ko V I, Colombo L, et al. A roadmap for graphene [J]. Nature, 2012, 490(7419): 192-200.

[2] Novoselov K S, Geim A K, Morozov S V, et al. Electric field effect in atomically thin carbon films [J]. Science, 2004, 306(5696): 666-669.

[3] Chen Z, Ren W, Gao L, et al. Three-dimensional flexible and conductive interconnected graphene networks grown by chemical vapour deposition [J]. Nature Materials, 2011, 10(6): 424-428.

[4] Yang W, Chen G, Shi Z, et al. Epitaxial growth of single-domain graphene on hexagonal boron nitride [J]. Nature Materials, 2013, 12(9): 792-797.

[5] Wei G. The chemistry of graphene oxide [M]// Graphene oxide. Cham: Springer International Publishing, 2015: 61-95.

[6] Mkhoyan K A, Contryman A W, Silcox J, et al. Atomic andelectronic structure of graphene-oxide[J]. Nano Letters, 2009, 9(3): 1058-1063.

[7] Pei S F, Cheng H M. The reduction of graphene oxide[J]. Carbon, 2012, 50(9): 3210-3228.

[8] Gilje S, Han S, Wang M S, et al. Achemical route to graphene for device applications [J]. Nano Letters, 2007, 7(11): 3394-3398.

[9] Wei Z, Wang D, Kim S, et al. Nanoscale tunable reduction of graphene oxide for graphene electronics [J]. Science, 2010, 328(5984): 1373-1376.

[10] Wan Z F, Streed E W, Lobino M, et al. Laser-reduced graphene: synthesis, properties, and applications [J]. Advanced Materials Technologies, 2018, 3(4): 1700315.

[11] Arul R, Oosterbeek R N, Robertson J, et al. The mechanism of direct laser writing of graphene features into graphene oxide films involves photoreduction and thermally assisted structural

rearrangement[J]. Carbon, 2016, 99: 423-431.

[12] Wan Z F, Wang S J, Haylock B, et al. Tuning the sub-processes in laser reduction of graphene oxide by adjusting the power and scanning speed of laser[J]. Carbon, 2019, 141: 83-91.

[13] Zhang Y L, Guo L, Wei S, et al. Direct imprinting of microcircuits on graphene oxides film by femtosecond laser reduction[J]. Nano Today, 2010, 5(1): 15-20.

[14] Gao W, Singh N, Song L, et al. Direct laser writing of micro-supercapacitors on hydrated graphite oxide films[J]. Nature Nanotechnology, 2011, 6(8): 496-500.

[15] Kurra N, Jiang Q, Nayak P, et al. Laser-derived graphene: a three-dimensional printed graphene electrode and its emerging applications[J]. Nano Today, 2019, 24: 81-102.

[16] Ke W M, Li Z H, Zhou Z X, et al. Reduced graphene oxide-based interferometric fiber-optic humidity sensor[J]. Acta Optica Sinica, 2019, 39(12): 1206007.
柯伟铭, 李振华, 周智翔, 等. 基于还原氧化石墨烯的干涉型光纤温度传感器[J]. 光学学报, 2019, 39(12): 1206007.

[17] Ni J, Wang C, Zhang C, et al. Three-dimensional chiral microstructures fabricated by structured optical vortices in isotropic material[J]. Light: Science & Applications, 2017, 6(7): e17011.

[18] Wang C, Yang L, Hu Y, et al. Femtosecond Mathieu beams for rapid controllable fabrication of complex microcages and application in trapping microobjects[J]. ACS Nano, 2019, 13(4): 4667-4676.

[19] Wang A D, Jiang L, Li X W, et al. Mask-free patterning of high-conductivity metal nanowires in open air by spatially modulated femtosecond laser pulses[J]. Advanced Materials, 2015, 27(40): 6238-6243.

[20] Kuchmizhak A A, Porfirev A P, Syubaev S A, et al. Multi-beam pulsed-laser patterning of plasmonic films using broadband diffractive optical elements[J]. Optics Letters, 2017, 42(14): 2838-2841.

[21] Cheng J, Gu C, Zhang D, et al. High-speed femtosecond laser beam shaping based on binary holography using a digital micromirror device[J]. Optics Letters, 2015, 40(21): 4875-4878.

[22] Liu S Y, Zhang J Y. Principles and applications of ultrafast laser processing based on spatial light modulators[J]. Laser & Optoelectronics Progress, 2020, 57(11): 111431.
刘思垣, 张静宇. 基于空间光调制器的超快激光加工原理及应用[J]. 激光与光电子学进展, 2020, 57(11): 111431.

[23] Wu P C, Zhang C C, Yang L, et al. Femtosecond laser dual-mode rapid fabrication based on spatial light modulator[J]. Chinese Journal of Lasers, 2018, 45(10): 1001005.
吴培超, 张晨初, 杨亮, 等. 基于空间光调制器的飞秒激光双模式快速加工[J]. 中国激光, 2018, 45(10): 1001005.

[24] Li B H, Jiang L, Li X W, et al. Flexible gray-scale surface patterning through spatiotemporal-interference-based femtosecond laser shaping[J]. Advanced Optical Materials, 2018, 6(24): 1801021.

[25] Zhang C C, Hu Y L, Du W Q, et al. Optimized holographic femtosecond laser patterning method towards rapid integration of high-quality functional devices in microchannels[J]. Scientific Reports, 2016, 6(1): 33281.

[26] Cheng H H, Liu J, Zhao Y, et al. Graphene fibers with predetermined deformation as moisture-triggered actuators and robots[J]. Angewandte Chemie, 2013, 125(40): 10676-10680.

[27] Yeh T F, Syu J M, Cheng C, et al. Graphite oxide as a photocatalyst for hydrogen production from water[J]. Advanced Functional Materials, 2010, 20(14): 2255-2262.

Patterned Graphene Oxide by Spatially-Shaped Femtosecond Laser

Guo Heng[1], Yan Jianfeng[1*], Li Xin[2], Qu Liangti[1,3]

[1] *Department of Mechanical Engineering, Tsinghua University, Beijing* 100084, *China;*

[2] *School of Mechanical Engineering, Beijing Institute of Technology, Beijing* 100081, *China;*

[3] *Department of Chemistry, Tsinghua University, Beijing* 100084, *China*

Abstract

Objective Graphene oxide (GO) is a graphene derivative with oxygen-containing functional group in its graphite structure. It can be reduced by heat, chemical reaction, and laser-induced reduction methods. Laser irradiation can induce reduction of GO in the irradiation area with good flexibility and area selectivity, and no special environment is required. In this paper, we propose a patterning method to process GO using a spatially-shaped femtosecond laser. We use the spatially-shaped laser irradiating method and a Gaussian laser scanning method to fabricate patterns on GO, and we analyze the effects of irradiation time, laser fluence, etc. The characteristic results demonstrate that the spatially-shaped femtosecond laser irradiating method realizes reductive patterning on GO, and the efficiency of patterning is improved. The proposed method also demonstrates good repeatability and flexibility in patterning. It has application potential in fabricating GO-based microcircuits and microdevices.

Methods GO films were prepared by filtering GO dispersion with a cellulose filter membrane and drying. The femtosecond laser has an 800-nm central wavelength, 35-fs pulse duration, and 1-kHz repetition rate. Different holograms were loaded on a spatial light modulator (SLM) to obtain the corresponding optical field at the focus. The Gerchberg-Saxon algorithm was used to calculate the phase distribution (i.e., hologram) according to the targeted complex amplitude distribution. When the specific optical field shape at the back focal plane of lens was obtained, the $4f$ optical system was used to guarantee that laser propagates without distortion and focuses on the surface of GO by the 5× objective lens. To realize unshaped laser scanning and compare fabrication results of shaped laser irradiating, a plane phase hologram was loaded on the SLM. Under this condition, an unshaped Gaussian optical field was formed at the focus. After reductive patterning, a scanning electron microscope (SEM) was used to characterize the micromorphology of the patterned areas to confirm the patterning effect of the two fabrication procedures. The height distribution and uniformity of the patterns were observed using a white light interferometer (WLI). Raman spectroscopy was used to obtain the Raman spectra of the patterned areas, and the characteristic peaks in the Raman spectra demonstrated whether the patterned area was reduced by the femtosecond laser.

Results and Discussions The two methods were used to fabricate the same four 40 mm × 40 mm square patterns on GO. Sketch maps of the two methods and micromorphologies characterized by SEM and WLI of the squares are showed (Fig. 2). For the proposed irradiating method, the intensity of the light field in the entire irradiating area was not uniform, and we regarded it as uniform when calculating fluence. The results demonstrate that the patterns are divided into many out-of-shape areas by gully-like structures. Areas surrounded by gullies showed hump-like structures (~5 μm scale). Some lamellar structures were observed on these humps. These results were generated by the nonuniform intensity of the optical field, gullies were fabricated by a light field with higher intensity, and humps were fabricated by a weaker light field. For the micromorphology of the laser scanning method, humps and gullies were also observed in the areas. However, the generated humps were smaller (~1 μm scale). Floccule structures were also observed in the entire area. These floccule structures were generated because gas was released from GO in a short period during laser scanning, which made the GO porous. Regarding fabrication efficiency, the irradiating procedure was performed in 500 ms; however, the scanning procedure required 640 s. We studied the influences of laser fluence and irradiating time on shaped laser irradiating (Fig. 3). Patterns irradiated with the same irradiating time and different fluence are distinguished on the depth and width of gullies. The D-band intensity of the Raman spectra indicates distortion of the graphic structure of GO, and 2D-band of the Raman spectra represents production of the graphene-like sp^2 structure. For unshaped laser scanning, we also adjusted some parameters to obtain diverse micromorphologies and reduction results (Fig. 4). Based on the Raman spectrum results, the maximum reduction in the two series of experiments was similar; however, the time required to perform each method differed significantly. Processing efficiency was improved significantly using shaped laser irradiating when we

fabricated the same pattern and obtained the nearly reduction effect. Finally, we applied the proposed spatially-shaped laser irradiating method to fabricate a "THU" shaped pattern (Fig. 5). For this relatively complicated pattern, it is difficult to fabricate it once via irradiation using the shaped laser because the calculation of the hologram would differ. The tailoring and splicing method can simplify this process. In this example, the entire pattern "THU" was difficult to fabricate directly; thus, we divided it into three parts, i.e., "T," "H," and "U," and we calculated their individual holograms. We then loaded the three holograms on the SLM and irradiated GO one after another.

Conclusions In this study, we have proposed a method based on spatial beam shaping technology and the G-S algorithm to realize reductive patterning on GO. The proposed method is compared with the Gaussian laser scanning method. The micromorphologies of patterns fabricated by the two methods are different. Gullies and big humps (~5 μm) were observed in areas irradiated by the shaped laser, and lamellar structures were observed on the humps. In areas scanned by the unshaped laser, the humps were smaller (~1 μm), and there were many floccule structures in these areas. Morphology observations demonstrate that the spatially-shaped laser irradiating method has good repeatability, and the final pattern does not change if the holograms loaded on the SLM are the same. Raman spectra demonstrate the reduction effect of the two methods. Longer irradiation time and larger fluence lead to better reduction effect in spatially-shaped laser irradiating procedure. Similarly, shorter scanning speed and larger fluence lead to reduction in laser scanning method. By adjusting related parameters, we obtained similar reduction extent in both methods. Here, the efficiency of the shaped laser irradiating was approximately 400 times that of the unshaped laser scanning. Finally, we applied the spatially-shaped laser irradiating method to fabricating more complicated patterns by tailoring and splicing the entire pattern, and the results confirmed the good flexibility of the proposed method. With improved efficiency and good repeatability and flexibility, the proposed method is expected to be applicable to the fabrication of GO-based microcircuits, microdevices, and many other related devices.

Key words laser technique; femtosecond laser; spatial pulse shaping; graphene oxide; patterning

OCIS codes 320.7090; 320.5540; 320.7130